Journal of Applied Polymer Science

Catalyzing Carbonization of Organophilic Alpha-Zirconium Phosphate/ Acrylonitrile-Butadiene-Styrene Copolymer Nanocomposites

Dan-Dan Yang,[1] Yuan Hu,[2] Hai-Ping Xu,[1] Lu-Ping Zhu[1]

[1]Department of Functional Materials, School of Urban Development and Environmental Engineering, Shanghai Second Polytechnic University, Shanghai 201209, China

[2]State Key Laboratory of Fire Science, University of Science and Technology of China, Hefei 230027, Anhui, China

Correspondence to: D.-D. Yang (E-mail: ddyang@sspu.cn)

ABSTRACT: The catalyzing carbonization function of alpha-zirconium phosphate (α-$Zr(HPO_4)_2 \cdot H_2O$, α-ZrP) based acrylonitrile-butadiene-styrene copolymer (ABS) is studied. Structure and morphology of the organophilic alpha-zirconium phosphate (OZrP)/ABS nanocomposites via melting interaction are characterized by X-ray diffraction (XRD) and high resolution transmission electron microscopy (HRTEM). The results indicate that a nanostructure is formed. The thermal stability of OZrP/ABS nanocomposites is investigated by thermogravimetric analysis (TGA). It is found that there is a transformation of the char microstructure in the ABS matrix with the OZrP. Morphology and structure (HRTEM and SAED) investigation distinctly show us the presence of graphite sheets and carbon nanotubes (CNTs) in the chars. Based on this found, a possible and reasonable mechanism of catalyzing carbonization is given in the discussion. © 2013 Wiley Periodicals, Inc. J. Appl. Polym. Sci. 130: 3038–3042, 2013

KEYWORDS: composites; catalysts; copolymers; thermal properties

Received 12 November 2012; accepted 25 February 2013; published online 11 April 2013
DOI: 10.1002/app.39224

INTRODUCTION

Novel attention is recently paid to synthesis of CNTs starting from polymers as carbon sources, which offers the additional advantages of energy-saving and environmental protection.[1–5] In addition, the possibility of improving thermal stability of polymer nanocomposites through catalyzing carbonization of the polymer itself during pyrolysis is investigated.[6,7] If CNTs or graphitic structure can be formed *in situ* during pyrolysis of polymer nanocomposites, the thermal stability of the polymer nanocomposites might be improved through reducing or stopping evaporation of gaseous flammable components.[8,9] In this regard, we demonstrate a novel method of synthesizing carbon nanotubes by catalytic pyrolysis of OZrP/ABS nanocomposites. α-ZrP, a layered phosphate, plays an important role in intercalation chemistry.[10,11] The protons between layers can exchange with many cations. α-ZrP is organified by a cationic surfactant before melt intercalation by ABS. The surfactant is an ammonium salt bearing long alkyl chains [hexadecyl trimethyl ammonium bromide (C16)]. OZrP obtains the trend to intercalate with polymer. In our previous study we had demonstrated that α-ZrP as a solid acid can be of the catalysis in the polymer dehydrogenation. α-ZrP was used in intumescent flame-retardant PP systems as synergistic agent, and graphite structure was founded in the chars of the intumescent flame-retardant OZrP/PP nanocomposites after the thermal decomposition.[12]

On the other hand, ABS is widely used as an important engineering thermoplastic because it has many attractive properties such as good processability, chemical resistance, and low cost. However, ABS also has several drawbacks, such as low thermal stability and poor flame retardancy.[13] The conventional flame retardants for ABS is halogen-containing compounds that leads to environmental problems by generating great quantities of toxic and corrosive fumes during combustion.[14,15] Recently, graphite is used to improve fire retardancy of ABS, and graphite offers the reduction in the peak heat release rate (PHRR) as measured by cone calorimetry.[16,17] In addition, transition metal chlorides (e.g., chlorides of chromium, iron, nickel, manganese, copper and tin etc.) are frequently used as catalyst at present,[8,9] and other forms of catalyst such as layer phosphates, have proved to be efficiency for carbonization and graphitization of ABS. Therefore, in this work, we study the catalyzing carbonization of the ABS itself in the presence of α-ZrP during pyrolysis. The results show that the loading of α-ZrP promotes the charred residue yield and CNTs can be obtained at relatively low temperatures ($\leq$800°C). Graphite sheets and CNTs are yielded even when the heat-treated temperature is less than

Table I. Compositions of the ABS Nanocomposites

Samples	Compositions
ABS0	Pure ABS
ABS1	ABS + 1 wt % OZrP
ABS2	ABS + 2 wt % OZrP
ABS3	ABS + 3 wt % OZrP

400°C. The possible catalyzing carbonization mechanism is also discussed in this paper.

EXPERIMENTAL

Materials

ABS was supplied as pellets by Dow Chemical (China) and the polymer was used as received. C16 was acquired from Shanghai Chemistry Co. OZrP was prepared by cation exchange of natural counterions with ammonium surfactants according to the method of Zhang et al.[18]

Instrumentation

XRD analysis was carried out on ABS nanocomposites at room temperature using a Japan Rigaku D/max-Ra X-ray diffractometer (30 kV, 10 mA) with Cu ($\lambda = 0.154178$ nm) irradiation at of 2° min^{-1} in the range of 1.5°–10°.

HRTEM images and selected area electron diffraction (SAED) patterns were obtained with a JEOL2010 microscope at an acceleration voltage of 200 kV. The HRTEM specimens were cut at room temperature using an ultramicrotome (Ultracut-1, UK) with a diamond knife from an epoxy block with the films of the nanocomposite embedded. Thin specimens (50–80 nm) were collected in a trough filled with water and then placed on 200 mesh copper grids.

The samples were analyzed by TGA using a Netzsch STA-409c Thermal Analyser at a temperature from 50 to 700°C using a linear heating rate of 10°C/min under an air flow of 50 cm^3/min. The mass of sample was about 10 mg.

Preparation

In our present work, OZrP was prepared by cation exchange of natural counterions with ammonium surfactants (C16). The OZrP and the ABS pellets were dried under vacuum at 80°C for overnight before using. A Brabender mixer of 50 g capacity was used for the preparation of all samples at 180°C for 10 min at 90 rpm. During the blending procedure, the OZrP powder was added directly to hot and melted ABS. Table I shows the mixing weight ratio of the samples. The prepared sample above (about 3 g) was put into an alumina crucible in a muffle furnace in a static air atmosphere at 360°C ~ 800°C for 1 h. After persistent heating, we obtained the carbonization products. The obtained carbonization products were ground in a pestle and mortar.

RESULTS AND DISCUSSION

Structure of OZrP/ABS Nanocomposites

Figure 1 shows the XRD patterns of (a) OZrP, (b) ABS1 (1 wt % OZrP/ABS nanocomposites) and (c) ABS3 (3 wt % OZrP/ABS nanocomposites). The maximum peak corresponds to the (002) plane reflection of the phosphate. The d_{002} peak of

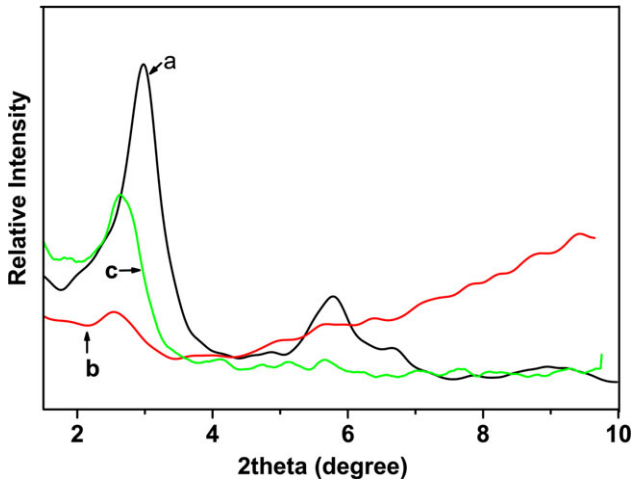

Figure 1. XRD patterns of (a) OZrP, (b) ABS1, and (c) ABS3. [Color figure can be viewed in the online issue, which is available at wileyonlinelibrary.com.]

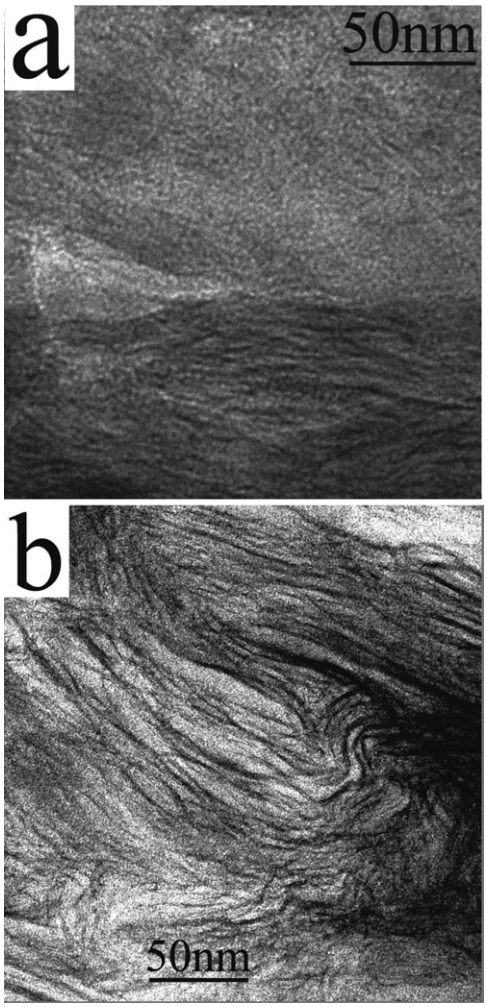

Figure 2. HRTEM images of OZrP/ABS nanocomposites: (a) ABS1 and (b) ABS3.

Applied Polymer SCIENCE

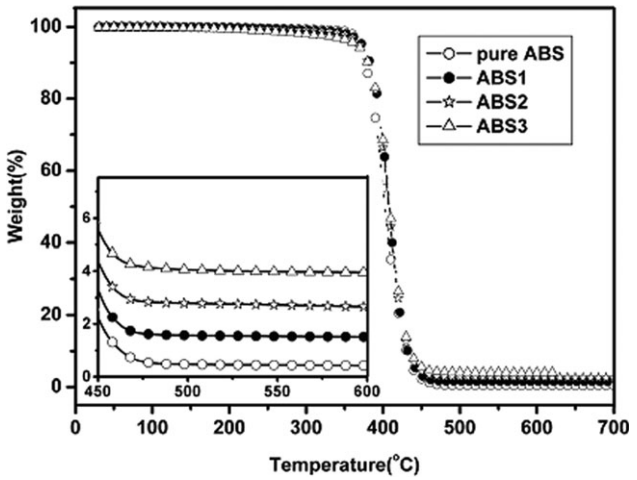

Figure 3. TGA curves of pure ABS and OZrP/ABS nanocomposites.

the α-ZrP at $2\theta = 11.6°$ corresponds to 0.76 nm interlayer spacing.[19,20] The XRD patterns indicate that the d_{002} peak of the OZrP, the corresponding interlayer spacing of which is 3.0 nm, is observed at lower angle ($2\theta = 2.9°$) than that of the α-ZrP [Figure 1(a)]. The increased spacing suggests the molecules of C16 intercalate into the gallery of α-ZrP. The XRD pattern of ABS3 [Figure 1(c)] shows that the average basal spacing of the phosphate layers increases from 3.0 nm of the OZrP to 3.4 nm. For ABS1 [Figure 1(b)], it shows that the d_{002} peak disappears. The reasons may be that ABS intercalates into the phosphate layers during the molten process, and it forms intercalated or exfoliated nanocomposites.

In this study, ABS1 and ABS3 are selected for high resolution electronic microscope observations to further confirm the dispersion of phosphate in the ABS matrix. The HRTEM images (Figure 2) indicate the OZrP is partly intercalated and partly exfoliated in samples, which is in accord with the XRD. Images show that phosphates, along with several layer stacks, are well-dispersed (intercalated or exfoliated) in the ABS matrix. The phosphates disperse in a regular manner, which may be due to the shear flow in melt extrusion.

Thermal Stability Property of the OZrP/ABS Nanocomposites

Thermal stability is an important property of composites. The kind, size, and concentration of filler have great influence not only on the morphology of composites, but also on the thermal stability of it. The thermal stability of pure ABS and the OZrP/ABS nanocomposites is analyzed by TGA. The TGA curves are shown in Figure 3. The 5 % weight loss temperature ($T_{-5\ wt\%}$), the maximum weight loss temperatures (T_{max}) and char residue at 600°C are listed in Table II. The results indicate that the onset of degradation for the OZrP/ABS nanocomposites occurs at a slightly lower temperature than the pure ABS. As for OZrP/ABS nanocomposites, the thermal stability does not

Table II. Thermal Stability Properties of the Pure ABS and OZrP/ABS Nanocomposites

Samples	$T_{-5wt\%}$ (°C)	T_{max} (°C)	Char residue (600°C, wt %)
ABS0	382.4	415.1	0.4
ABS1	381.1	414.6	1.5
ABS2	378.2	415.3	2.8
ABS3	376.4	414.4	4.1

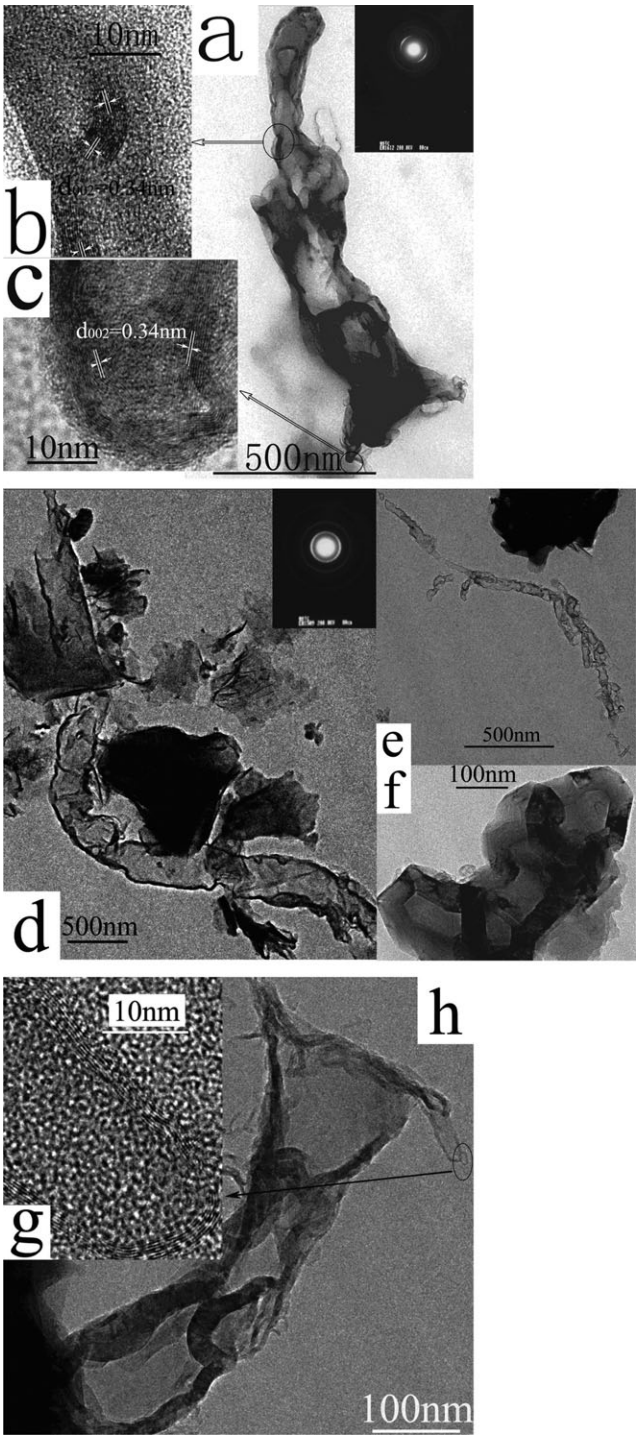

Figure 4. HRTEM images and SAED patterns of ABS3: (a, b, c) the char residue at 360 °C, (d, e, f, g, h) the char residue at 500 ~ 800°C.

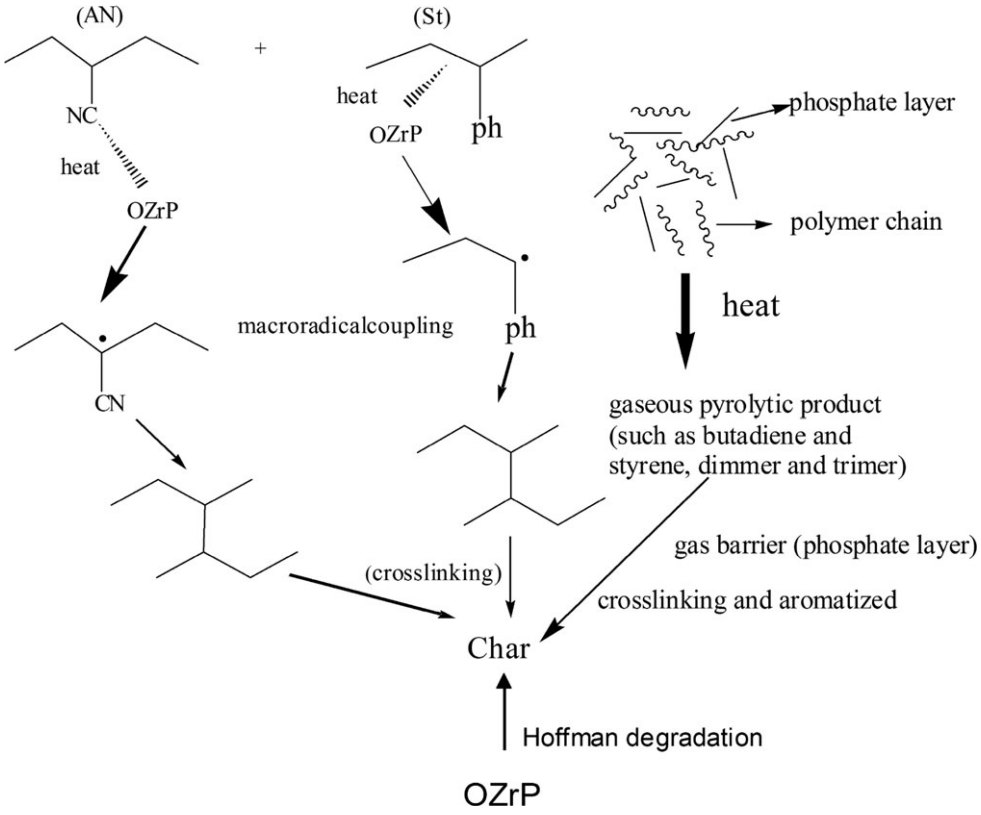

Scheme 1. Schematic figures of the possible catalyzing carbonization models of OZrP/ABS nanocomposites.

remarkably increase compared to pure ABS. This is partly caused by the Hoffmann elimination reaction of C16 at lower temperature. This may be also that the OZrP catalyze the degradation of ABS matrixes.

As the OZrP content increase from 1 to 3 wt %, the amount of charred residue increases at 600°C. This means that OZrP promotes charring to form a carbonaceous material. The detailed catalyzing carbonization mechanism will be discussed in the following part.

Structure Analysis of the Charred Residue of OZrP/ABS Nanocomposites

The observation of HRTEM for nanostructures of the charred residue from combustion of ABS3 (3 wt % OZrP/ABS) nanocomposites at 360°C ~ 800°C displays that the charred residue possesses graphite sheets and CNTs (Figure 4). There are some poor crystallized multi-walled carbon nanotubes (MWCNTs) from combustion of ABS3 nanocomposites at 360°C in Figure 4(a). Despite of there being many defect structures (such as dislocation and cavity) and amorphous (outside walls) structures, the graphitic character can be observed in the walls of MWCNTs from the images of HRTEM [Figure 4(b,c)]. When the combustion temperature increases, more well-crystallized CNTs and graphite sheets are yielded from 500°C to 800°C [Figure 4(d–f,h)]. The SAED patterns [Figure 4(a,g)] reveal the polycrystalline nature of the CNTs. Figure 4(h) shows a piece of graphite sheet, and its edges are curled into tubes. The graphitic character also can be observed in the walls of MWCNTs from the image of HRTEM [Figure 4(g)]. The main diameters of CNTs are about 50–500 nm. There are also a wide range of the lengths of CNTs, and the longest CNT is about 2 μm.

In general, the combustion of pure polymers includes degradation of polymers and combustion of degradation products. The former is a solid-phase reaction, and the latter is gas-phase reaction. When the temperature is high enough, the exterior polymer will stand oxidative degradation due to existence of oxygen and the inside polymer will thermally degrade via radical mechanism due to absence of oxygen. However, thermal degradation of the inside polymers may be changed, for example, catalytic degradation of polymers may occur in the presence of acid catalyst (such as solid acids). First, the OZrP is a solid acid. OZrP can thermally loose H^+, which will attack molecular chains of ABS to form cationic active sites, and results in catalytic degradation of ABS and yields macroradicals. Moreover, OZrP also possesses other Lewis acid sites, namely, Zr^{4+}. Lewis acid sites Zr^{4+} can further catch those macroradicals to recombine and leads to the intermolecular crosslinking. In the next place, at the present of layer phosphate, a protective charred ceramic surface layer is formed as the result of the ablative reassembly of the phosphate layers on the polymer surface and the OZrP catalyzes charring ABS, which lowers the diffusion rate of the inside pyrolytic products.[21] The inner OZrP layers within ABS nanocomposites also prevent the gaseous pyrolytic products from volatilization. The gas barrier properties of layer phosphate form a maze or "tortuous path" and these pyrolytic products will have more time to contact OZrP and are dehydrogenated

and aromatized to form char containing graphite sheets and CNTs.[22] Thus, the monomers such as butadiene and styrene, dimmers and trimers coming from the ABS chain scission are sealed with an ABS matrix, crosslinked and aromatized to formed graphite sheets and CNTs. The scheme of the catalyzing carbonization mechanism for OZrP/ABS nanocomposites is shown in Scheme 1.

CONCLUSIONS

In summary, OZrP/ABS nanocomposites were synthesized by melt mixed. XRD, HRTEM and TGA were carried out to characterize the morphology and properties of the nanocomposites. The results show that nanocomposites have partly intercalated and partly exfoliated structures. OZrP plays the role of a catalyst. The structure and morphology of the charred residue approve further the presence of graphite sheets and CNTs. Graphite sheets and CNTs are yielded even when the heat-treated temperature is less than 400°C. During the synthesis process for formation of graphite sheets and CNTs, acidic sites on the degraded phosphate layers and the protective charred ceramic surface layer have changed the mechanism of degradation reaction of ABS from thermal degradation to catalytic degradation, which leads to more degradation products easily catalyzed and promotes the yield of graphite sheets and CNTs. The results of this article indicate possibilities for important future developments in the field of catalyzing carbonization of polymers.

REFERENCES

1. Schmalz, T.; Kraus, T.; Gunthner, M.; Liebscher, C.; Glatzel, U.; Kempe, R.; Motz, G. *Carbon* **2011**, *49*, 3065.
2. Yu, H. O.; Kashiwagi, T.; Tang, T. *Polymer* **2009**, *50*, 6252.
3. Kong, Q. H.; Zhang, J. H. *Polym. Degrad. Stab.* **2007**, *92*, 2005.
4. Tang, T.; Chen, X. C.; Meng, X. Y.; Chen, H.; Ding, Y. P. *Angew. Chem. Int. Ed.* **2005**, *44*, 1517.
5. Gong, J.; Liu, J.; Ma, L.; Wen, X.; Chen, X. C.; Wan, D.; Yu, H. O.; Jiang, Z. W.; Borowiak-Palen, E.; Tang, T. *Appl. Catal. B: Environ.* **2012**, *117*, 185.
6. Cai, Y. B.; Huang, F. L.; Wei, Q. F.; Song, L.; Hu, Y.; Ye, Y.; Xu, Y.; Gao, W. D. *Polym. Degrad. Stab.* **2008**, *93*, 2180.
7. Lu, H. D.; Song, L.; Hu, Y. *Polym. Adv. Technol.* **2011**, *22*, 379.
8. Cai, Y. B.; Hu, Y.; Song, L.; Xuan, S. Y.; Zhang, Y.; Chen, Z. Y.; Fan, W. C. *Polym. Degrad. Stab.* **2007**, *92*, 490.
9. Tang, T.; Chen, X. C.; Chen, H.; Meng, X. Y.; Jiang, Z. W.; Bi, W. G. *Chem. Mater.* **2005**, *17*, 2799.
10. Taniguchi, M.; Yamagishi, A.; Iwamoto, T. *J. Phys. Chem.* **1990**, *94*, 2534.
11. Christensen, A. N.; Andersen, E. K.; Anderen, I. G. K. *Acta Chem. Scand.* **1990**, *44*, 865.
12. Yang, D. D.; Hu, Y.; Song, L.; Nie, S. B.; He, S. Q.; Cai, Y. B. *Polym. Degrad. Stab.* **2008**, *93*, 2014.
13. Feyz, E.; Jahani, Y.; Esfandeh, M. *J. Appl. Polym. Sci.* **2011**, *120*, 3435.
14. Costa, L.; Camino, G.; Bertelli, G. *Polym. Degrad. Stab.* **1991**, *34*(1/3), 55.
15. Carty, P.; White, S. *Polym. Degrad. Stab.* **1995**, *47*, 305.
16. Uhl, F. M.; Yao, Q.; Wilkie, C. A. *Polym. Adv. Technol.* **2005**, *16*, 533.
17. Ge, L. L.; Duan, H. J.; Zhang, X. G.; Chen, C.; Tang, J. H.; Li, Z. M. *J. Appl. Polym. Sci.* **2012**, *126*, 1337.
18. Zhang, R.; Hu, Y.; Wang, S. L. *Rare Metal Mater. Eng.* **2006**, *35*(S2), 100.
19. Troup, J. M.; Clearfield, A. *Inorg. Chem.* **1977**, *16*, 3311.
20. Albertsson, J.; Oskarsson, A.; Tellgren, A.; Thomas, J. O. *J. Phys. Chem.* **1977**, *81*, 1574.
21. Zanetti, M.; Kashiwagi, T.; Falqui, L.; Camino, G. *Chem. Mater.* **2002**, *14*, 881.
22. Lewin, M.; Endo, M. *Polym. Adv. Technol.* **2003**, *14*, 3.